

DOI: 10.1515/amm-2017-0100

K. LYCZKOWSKA\*<sup>#</sup>, J. MICHALSKA\*\*

## STUDIES ON THE CORROSION RESISTANCE OF LASER-WELDED INCONEL 600 AND INCONEL 625 NICKEL-BASED SUPERALLOYS

The paper presents the results of the electrochemical corrosion tests of Inconel 600 and Inconel 625 laser-welded superalloys. The studies were conducted in order to assess the resistance to general and pitting corrosion in 3.5% NaCl solution. It was found that Inconel 600 possesses good corrosion resistance, however Inconel 625 is characterized by a greater resistance to general and also to pitting corrosion of the weld as well as the base metal.

*Keywords:* electrochemical corrosion; Inconel 600; Inconel 625; pitting corrosion; laser welding

### 1. Introduction

Owing to the increased demand for power in the world, it is necessary to search for new and cheaper sources of electricity and to modify the existing ones. The European Union strives for the reduction of greenhouse gas emission, the effect of which is the application of boilers of higher operating parameters to increase their effectiveness to over 50% [1]. It is necessary to modernize the equipment in use and to construct new power units with supercritical and ultra supercritical parameters, in order to comply with the EU directives [2]. This requires the application of materials of better properties, which is why one conducts studies on the materials of high heat resistance and high-temperature creep resistance and their welded joints. Hence the need for research on materials that will meet the requirements of corrosive environments [3].

The material for heat exchanger tube needs to have good mechanical properties and good corrosion resistance, especially at high temperature condition assuring service lifetime for around 40 years. Inconel series alloys have been widely used as the material for power industry because of the advantageous properties of high strength and good workability with excellent corrosion resistance and a coefficient of thermal expansion (CTE) similar to that of low alloy steel. However, technical inspections and research reports revealed increasing tendency to corrosion of heat exchanger made of Inconel alloys, especially in their welded areas, where extensive pitting, intergranular attack and stress corrosion cracking have been observed [4-7].

Many of the Inconel alloy components deployed in power plants are fabricated using conventional arc welding processes. Such welding processes generate a tremendous amount of heat within the fusion zone (FZ) and heat-affected zone (HAZ) of the welded component, and thus "sensitization" may occur, what drastically reduces the corrosion resistance of the Inconel alloy weldments. Therefore, the power plant industries have been developing the laser beam welding technology, which may prevent harmful microstructural changes in the FZ and HAZ. Laser beam welding is a high-energy density, low heat-input process characterized by a higher welding speed, low residual stress and more rapid cooling rate [8,9]. One of the many advantages of laser beam welding is the capability to weld without filler metal and small FZ and HAZ zones. As a result, the mechanical performance of the weldment is considerably improved. Although excellent microstructural features, heat and mechanical properties of laser beam weldments, corrosion resistance is also one of the most important factors in evaluation of long term life service of Inconel alloys. Many authors postulated that evaluation of corrosion resistance is absolutely essential to prevent premature damages of weldments [10-12].

The current study presents the results on electrochemical corrosion studies of two Inconel series alloys: Inconel 600 and Inconel 625. The investigated alloys presented different chemical composition which may affect the structure of FZ and HAZ and hence their corrosion resistance. The aim of the study was to compare the corrosion resistance to general and pitting corrosion of laser welded Inconel 600 and 625 alloys including characteristics for the base metal and for the weldment.

\* SILESIAAN UNIVERSITY OF TECHNOLOGY, FACULTY OF MATERIALS ENGINEERING AND METALLURGY, INSTITUTE OF METALS TECHNOLOGY, 8 KRASIŃSKIEGO STR., 40-019 KATOWICE, POLAND

\*\* SILESIAAN UNIVERSITY OF TECHNOLOGY, FACULTY OF CHEMISTRY, DEPARTMENT OF INORGANIC CHEMISTRY, ANALYTICAL CHEMISTRY AND ELECTROCHEMISTRY, 6 KRZYWOUSTEGO STR., 44-100 GLIWICE, POLAND

<sup>#</sup> Corresponding author: katarzyna.lyczkowska@vp.pl

TABLE 1

Chemical compositions of investigated alloys (wt.-%)

Alloy	Cr	Mo	Fe	Mn	Cu	Nb	Ti+Al	C	Si	(S+P)	Ni+Co
600	14-17	—	6-10	1.0	0.5	—	—	0.15	0.5	0.015	72
625	20-23	8-10	5	0.4	—	3.15-4.15	0.8	0.10	0.5	0.030	58-61

## 2. Research methodology and material

The research materials were nickel-based superalloys Ni-Cr-Mo, Inconel 600 and Inconel 625. The nominal chemical compositions of investigated alloys are presented in Table 1.

Electrochemical tests were carried out in aerated 3.5% NaCl in accordance with the PN-EN ISO 17475:2010 standard. Potentiodynamic curves were recorded using a measuring system composed of a computer controlled Solartron 1287 potentiostat and traditional three-electrode cell, wherein the saturated calomel electrode (SCE) acted as a reference electrode and a platinum mesh as a counter electrode. The measuring procedure started with recording the OCP for 45 minutes. Next, the electrode potential was anodically scanned at a rate of 10 mV min<sup>-1</sup> from -300 mV vs. OCP up to the reaching breakdown potential  $E_b$ . Stern-Geary method within the range of potential  $\pm 10$  mV in relation to the OCP was applied to determine following parameters: corrosion potential  $E_{cor}$ , corrosion current density  $i_{cor}$  and polarization resistance  $R_p$ . The tendency towards pitting corrosion was assessed based on: breakdown potential of the passive layer  $E_b$  and passivity range  $\Delta E_1 = E_b - E_{cor}$ .  $E_b$  was termed as the potential at which a monotonic increase in the anodic current exceeding 25  $\mu\text{A cm}^{-2}$  occurred. The obtained results were elaborated by means of a Corrview 3.0 software. Samples were tested in triplicate.

Electrochemical studies were completed with microstructural (SEM) studies of corroded surfaces for the evaluation of corrosion attack morphology. For that purpose, Hitachi S-4300N SEM coupled with Thermo Noran EDS system was used. The imaging sites for SEM were randomly chosen on the specimen surface to be representative of the entire surface of the coupons.

## 3. Results and discussion

The results of electrochemical measurements in case of individual samples were presented in Table 2 and in Fig. 1. The general corrosion process progresses evenly over the entire surface of the tested material within the specified time. The corrosion potential ( $E_{cor}$ ) presents thermodynamic relations occurring in the course of a reaction between the tested material and the corrosive environment. A decreased corrosion resistance is usually associated with a shift of the corrosion potential  $E_{cor}$  towards the more cathodic values. However in the case of materials of high tendency to passivation, the values of  $E_{cor}$  do not reflect the kinetics of the corrosion process. Then, the kinetics of the corrosion processes is described by corrosion current density  $i_{cor}$ . When the general corrosion decreases, the resistance

current density  $i_{cor}$  increases, therefore the corrosion rate  $V_v$  is determined based on  $i_{cor}$  and the density of the tested material. At the same time the value of polarization resistance  $R_p$  (protective barrier) is decreased, which has a negative impact on the electrochemical properties of the material (corrosion resistance, passivation processes, breakdown potential).

TABLE 2

The results of electrochemical tests for the investigated superalloys

Sample	$E_{cor}$ [mV]	$R_p$ [k $\Omega$ cm <sup>2</sup> ]	$i_{cor}$ [ $\mu\text{A cm}^{-2}$ ]	$E_b$ [mV]	$\Delta E_1$ [mV]	
Inconel 600	base	-217	7964	0.033	357	574
		-273	50.6	0.516	337	610
		-287	2154	0.121	236	523
	weld	-233	2555	0.081	227	460
		-196	16.5	1.675	243	439
		-169	33.3	0.785	252	421
Inconel 625	base	-275	2715	0.096	377	652
		-220	5205	0.051	636	856
		-301	286	0.079	620	921
	weld	-191	1693	0.154	677	868
		-176	3059	0.085	898	1074
		-106	14.1	1.846	821	927

Comparing the electrochemical characteristics of investigated alloys it was clearly visible that Inconel 625 possessed higher corrosion resistance to general corrosion and pitting corrosion. Lower  $i_{cor}$  values, stable range of passivity and more noble values of  $E_{cor}$  were observed (Table 2, Fig. 1b) what is directly related to the chemical composition of superalloys. Inconel 625 possesses more alloying elements increasing the passivity and corrosion resistance of the alloy such as Cr, Mo and Nb.

It has been proved that welding process had impact on the resistance to general corrosion of the investigated alloys. Higher  $i_{cor}$  values and higher current densities within passive range on were recorded in comparison to the base materials. For the base material of Inconel 600  $i_{cor}$  values were in the range from 0.033 to 0.516  $\mu\text{A/cm}^2$ , while for the weld metal  $i_{cor}$  assessed values even 30 times higher: ranging from 0.081 to 1.675  $\mu\text{A/cm}^2$ . The same tendency was observed for Inconel 625. Distinctly higher values of  $i_{cor}$  were established for Inconel 625 weld metal (ranging from 0.085 to 1.846  $\mu\text{A/cm}^2$ ) compared to the base material of Inconel 625 (values 0.051 to 0.096  $\mu\text{A/cm}^2$ ). For all the samples coming from the Inconel 625 weld metal,  $E_{cor}$  values were shifted to the more anodic (more noble) direction in comparison to the base materials.

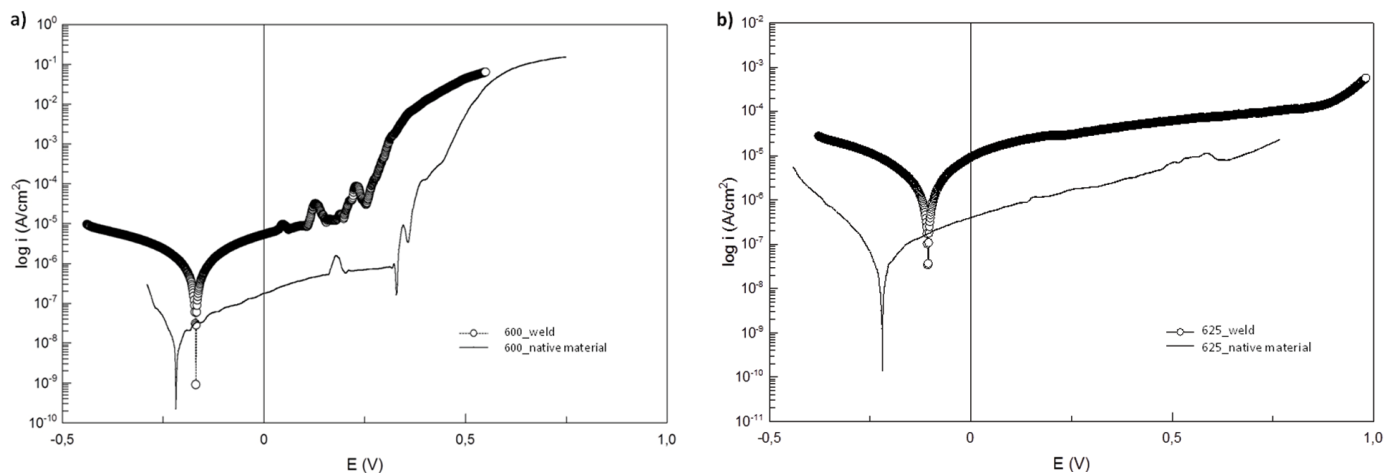


Fig. 1. Junxtaposition of potentiodynamic curves recorded in 3.5% NaCl for base material and weld of the superalloys: (a) Inconel 600 and (b) Inconel 625

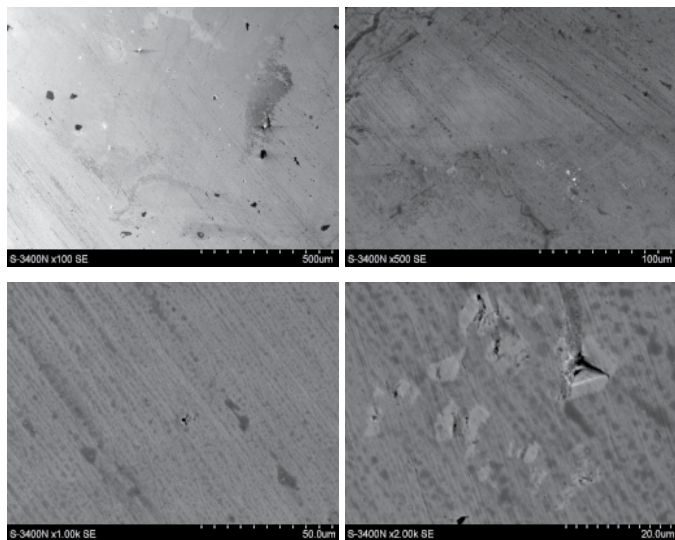


Fig. 2. Morphology of corrosion damage to the base material of the Inconel 625

The pitting corrosion was assessed by the  $E_b$  value, which describes a breakdown potential of the passive layer. It is established as a potential point at which a sudden increase in the current density is observed. The higher value of the  $E_b$ , the better resistance of the material against the development of pitting corrosion.

Investigated alloys showed different pitting resistance. As expected, lower corrosion resistance to pitting had Inconel 600 alloy. Passive layer on the base Inconel 600 alloy was distinctly broken down at potential range: 236–357 mV. Welding additionally decreased the corrosion resistance to pitting of Inconel 600 alloy. Lower values of  $E_b$  was observed (227–252 mV) and shorter ranges of passivity had been recorded for weld metal samples, respectively.

On the contrary, samples of Inconel 625 weld metal showed higher corrosion resistance to pitting compared to the base Inconel 625 material. For base material the passive range did not exceed 921 mV, and the highest recorded value of  $E_b$  was 636 mV. For the Inconel 625 weld metal, the highest value of  $E_b$  was

898 mV and the passive range values were even 218 mV wider than those obtained for Inconel 625 base material.

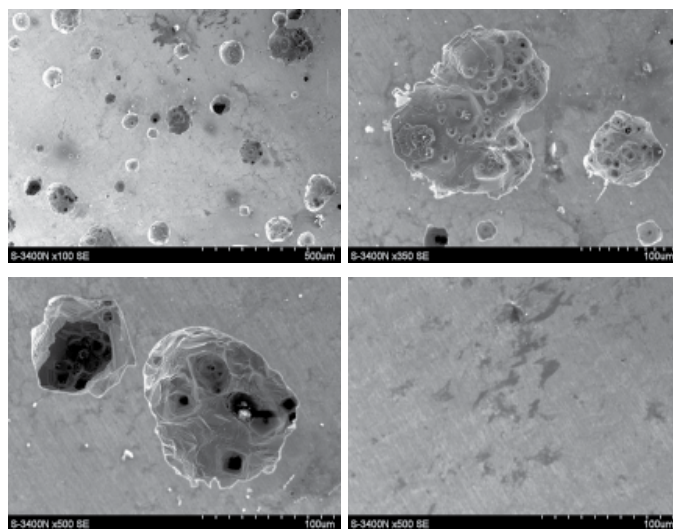


Fig. 3. Morphology of the corrosion damage in Inconel 600 weld metal

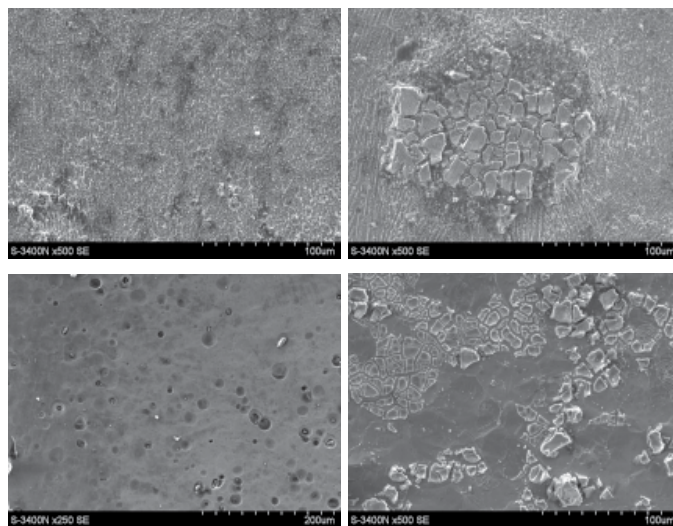


Fig. 4. Morphology of corrosion damage in Inconel 625 weld

Microscopic observations of samples' surface after polarization studies were in a good agreement with electrochemical analysis. There was no significant corrosion damage signs on the surface of both base materials (Fig. 2). Locally, small pits were observed on the surface. Most of the observed surface was free from any corrosion damage. The high resistance to corrosion displayed by the base materials is connected with their austenitic structure after the rolling process and equiaxed grains.

However, significant differences in the morphology of the damage caused by pitting corrosion was observed for the weld metals (Figs. 3 and 4).

Surface of the Inconel 625 weld metal was almost free from pits and crevices, uniform dissolution was mainly observed. Locally near to the HAZ zone, few small and shallow pits were observed. Locally, thin film of cracked NaCl layer was observed on the surface.

Aglomeration of small-size pits, numerous deep pitting as well as even an etching of the structure in the area of the grain boundaries were observed on the surface of Inconel 600 weld metal. Several deep corrosion pits of a diameter  $>50 \mu\text{m}$  were observed.

The discrepancy between the results obtained for the welds is probably related to the structure and heterogeneous chemical composition. At certain areas of the Inconel 600 weld, the corrosion process may occur more rapidly, which may be connected with the existence of areas of heterogeneous dendrites or impurities in the weld metal structure. Laser beam welding of Inconel 625 alloy assures welded joint with full penetration with more homogeneous chemical composition, a narrow heat-affected zone and a fusion weld area without any welding imperfections.

#### 4. Conclusions

Increased corrosion current density  $i_{\text{cor}}$  for all weldment samples were observed, nevertheless the values of the corrosion potential  $E_{\text{cor}}$  are slightly shifted towards the more noble values, as compared to the values obtained for the base material. Stern-Geary analysis and pitting corrosion evaluation had proved that Inconel 625 superalloy possessed the best electrochemical properties and corrosion resistance. The base material and the weldment of Inconel 625 showed lower current densities on polarization curves, wider and more stable passive range and higher values of breakdown potential guaranteeing good resistance to general and pitting corrosion in 3.5% NaCl solution.

#### Acknowledgements

The project was financed under the applied Research Programme funded by the National Centre for Research and Development, project entitled: "Technology of laser welding of finned tubes made of austenitic steel and nickel alloys designed for boilers with supercritical and ultra supercritical parameters", agreement no : PBS1/A5/13/2012.

#### REFERENCES

- [1] J. Adamiec, M. Więcek, G. Kokot, *Przegląd Spawalnictwa* **5**, 3-9 (2014).
- [2] J. Adamiec, B. Piliszko, *Inżynieria Materiałowa* **6**, 907-913 (2007).
- [3] A. Hernas, B. Kościelniak, J. Hajda, *Mikrostruktura i właściwości złączy spawanych z nadstopu niklu Inconel 740H po starzeniu w 750°C*, w: *Charakterystyki nowej generacji materiałów dla energetyki*, pod red. A. Hernasa, Bełchatów 175-176, 2015.
- [4] J. Dobrzański, *Materiałoznawcza interpretacja trwałości stali dla energetyki*, Open Access Library 3, 2011.
- [5] M. Drop, E. Włoczyk, *Materiały stosowane na urządzenia energetyczne. Teraźniejszość i przyszłość. Dozór techniczny* **1**, 9-15 (2006).
- [6] P.M. Scott, An overview of materials degradation by stress corrosion in PWRs, in: D. Feron, J.M. Olive (Eds.), *Corrosion Issues in Light Water Reactors: Stress Corrosion Cracking*, Woodhead, England 3-24, (2007).
- [7] T. Fujii, K. Sue, S.I. Kawasaki, *The Journal of Supercritical Fluids* **95**, 285-291(2014)
- [8] P. Berge, *Stress Corrosion Cracking of Nickel Based Alloys in Water-cooled Nuclear Reactors* 143-146, (2016).
- [9] J. Łabanowski, A. Świerczyńska, J. Michalska, *Solid State Phenomena* **227**, 267-270 (2015).
- [10] J. Michalska, J. Łabanowski, J. Cwiek, *Materials Science and Engineering IOP Conference Series* **35**, 012012 (2012) (doi.org/10.1088/1757-899X/35/1/012012)
- [11] H.T. Lee, J.L. Wu, *Corrosion Science* **51**, 733-743 (2009).
- [12] J. Brózda, G. Czaja, *Żarowytrzymała stal T92/P92, jej spawanie i własności złączy spawanych*, *Przegląd Spawalnictwa* **4**, 51-61 (2014).